Available online at www.sciencedirect.com
SCIENCE DIRECT
Polymer 46 (2005) 10173–10179
polymer
www.elsevier.com/locate/polymer

Low-temperature reactive coupling at polymer–polymer interfaces facilitated by supercritical CO_2

S.E. Harton[a], F.A. Stevie[b], R.J. Spontak[a,c], T. Koga[d], M.H. Rafailovich[d], J.C. Sokolov[d], H. Ade[e,*]

[a]*Department of Materials Science and Engineering, North Carolina State University, Raleigh, NC 27695, USA*
[b]*Analytical Instrumentation Facility, North Carolina State University, Raleigh, NC 27695, USA*
[c]*Department of Chemical and Biomolecular Engineering, North Carolina State University, Raleigh, NC 27695, USA*
[d]*Department of Materials Science and Engineering, State University of New York, Stony Brook, NY 11794, USA*
[e]*Department of Physics, North Carolina State University, Partners III Box 7518, 851 Main Campus Dr, Raleigh, NC 27695, USA*

Received 8 June 2005; received in revised form 19 July 2005; accepted 25 July 2005
Available online 22 August 2005

Abstract

Supercritical CO_2 ($scCO_2$) has been used to facilitate reactions in thin film bilayers between functionalized polystyrene and poly(methyl methacrylate) at temperatures far below the glass transition temperatures of the respective polymers. Secondary ion mass spectrometry (SIMS) is used to monitor the reaction progression directly by measuring the interfacial excess of deuterated PS. Complementary X-ray reflectometry (XR) yields the interfacial width and surface roughness of bilayer films for reactive systems with and without the addition of $scCO_2$, and comparisons are made with unreactive reference systems. From XR and SIMS analyses, the interfacial width and roughness have been found to be effectively independent of the reaction conditions employed here, and the primary impact of incorporated $scCO_2$ is enhanced mobility of the reactive polymer chains. The use of $scCO_2$ can change polymer mobility significantly enough over a very small temperature range ($\Delta T \sim 15$ °C) so that both diffusion- and reaction-controlled type behavior can be observed for otherwise identical systems.

Keywords: Polymer bends; Reactive compatibilization; Supercritical fluids

1. Introduction

Many current technologies and commercial products exploit the combined properties of multicomponent polymer systems [1]. Polymer mixtures typically possess unfavorable enthalpic interactions and a negligibly low entropy of mixing due to the long, chain-like nature of the molecules [2]. These two factors account for the general immiscibility encountered in polymer blends [3]. Mixing two immiscible polymers as viscoelastic liquids at elevated temperatures consequently results in liquid–liquid phase separation commonly signified by the formation of dispersions (micrometer size or larger) of one polymer in a matrix of the other [4,5]. These morphological features are frozen-in once the blend is cooled below the temperature at which one or both polymers vitrify. To overcome the inherent immiscibility of most polymer pairs, and thus capture the material properties of both polymers in a controllable and stable fashion, strategies have been developed to improve polymer–polymer compatibility through the addition of premade block copolymers (BCPs) [3,6,7], the formation of such BCPs via reactive compatibilization [8–10], and the use of supercritical CO_2 ($scCO_2$) [11–13].

Premade BCPs are routinely added as surfactants to compatibilize immiscible polymer blends, resulting in improved dispersion, adhesion, and long-term stability [14,15]. However, despite ongoing advances in synthesizing BCPs [15,16], few copolymers are commercially available and reactive coupling has become an attractive alternative to the use of premade BCPs. Reactive compatibilization is a robust means by which dissimilar polymers can be chemically coupled at elevated temperatures to form copolymer molecules in situ [8–10]. Specifically, functionalized polymers are physically blended and reacted as

* Corresponding author. Tel.: +1 919 1551 1331.
E-mail address: harald_ade@ncsu.edu (H. Ade).

0032-3861/$ - see front matter © 2005 Elsevier Ltd. All rights reserved.
doi:10.1016/j.polymer.2005.07.085

liquids at temperatures above their intrinsic glass transition temperatures (T_gs) (Fig. 1) to form linear or graft copolymer molecules at the polymer–polymer interface where they are most needed [14].

The importance of reactive coupling at highly immiscible polymer–polymer interfaces has resulted in a relatively large number of theoretical [17–25] and experimental [8,10,26–28] investigations to characterize the reaction kinetics as a function of molecular weight, functional group reactivity, and polymer mobility. Many recent experimental investigations of reactive coupling at interfaces commonly rely on planar films [26,27,29], where detection and quantitation of copolymer formation can be straightforward using real-space depth-profiling techniques [30,31]. Some studies [26,28,29] have concluded that the interfacial reactions examined, although involving highly reactive functional groups [32], appear to be reaction-controlled (RC). Direct observation of diffusion-controlled (DC) reactions has only recently been achieved through the observation of a depletion hole in a system of hydroxyl-terminated deuterated polystyrene (dPS–OH) and a random copolymer of methyl methacrylate and methacryloyl chloride (PMMA-*co*-MAA) annealed at 120 °C [27]. Numerous aspects of DC reactions, however, require further investigation to decouple the various influences on the reaction, including reactive polymer composition [33], interfacial width (reaction volume) [28], and changes in polymer mobility [34,35] due to possible changes in T_g near the interface [36]. Here, we provide direct evidence that reactive coupling can be achieved through the use of $scCO_2$ at temperatures substantially below the intrinsic T_gs of the polymers employed. The addition of specific amounts of $scCO_2$ introduces a polymer 'mobility knob' that controllably plasticizes the polymer (Fig. 1) resulting in observable RC- and DC-type behaviors over small variations in reaction temperature.

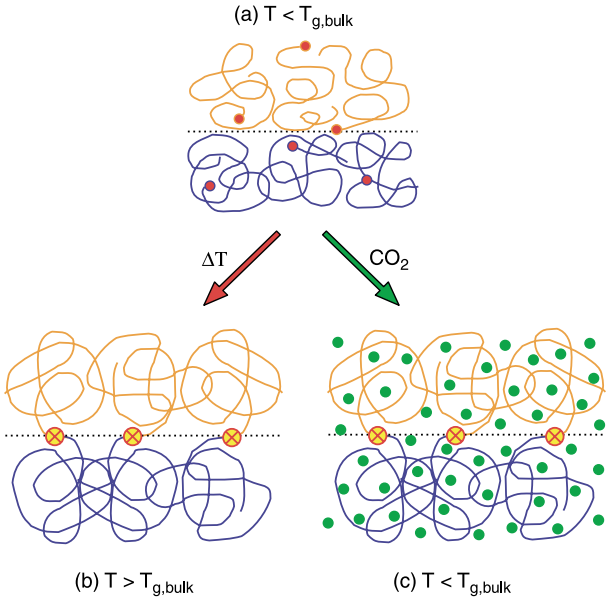

Fig. 1. Reactive coupling at an interface between end-functionalized amorphous polymers (a) produces diblock copolymers in situ when processed in (b) the melt or (c) $scCO_2$.

Hydrogenous and perdeuterated atactic polystyrene (PS and dPS, respectively) and syndiotactic poly(methyl methacrylate) (PMMA) are used as model polymers in this investigation, since they are completely amorphous and possess T_gs well above the critical temperature of CO_2. Amine ($–NH_2$) and acyl chloride (–COCl) functional groups are employed to couple these polymers in the presence of $scCO_2$, as this highly robust, irreversible condensation reaction is known to be extremely reactive at low-temperatures [37,38]. Deuterium depth profiles delineating the spatial distribution of dPS–COCl along the surface normal have been acquired using secondary ion mass spectrometry (SIMS) to directly observe and quantify the reaction product as an interfacial excess of dPS signal. In addition, effective interfacial widths (w) and surface roughnesses (σ) of reactive and unreactive PS/PMMA bilayers have been determined by X-ray reflectometry (XR) after exposure to $scCO_2$. A comparison is made to an analogous system annealed at high temperature under vacuum, using a reaction of –COCl and hydroxy (–OH) functional groups.

2. Experimental

2.1. Materials and sample preparation

All polymers were purchased from Polymer Source, Inc (Dorval, Canada). Their molecular weights, polydispersity indices, and degrees of functionality are listed in Table 1. According to differential scanning calorimetry (DSC), the inflection point T_gs (measured upon second heating) for the PS and PMMA were 104 and 128 °C, respectively. Five different bilayer systems (*A*–*F*) were produced as summarized in Table 2. The end groups of the PS used in systems *A*, *B* and *D* was first converted from –COOH to –COCl using well-established methods [39] before bilayer preparation. After dissolving either dPS–COOH or PS–COOH in anhydrous toluene, ~100× excess of oxalyl chloride was added and stirred for ~12 h under nitrogen. The solution was placed under vacuum at 25 °C to remove ~80% of the toluene and then precipitated in anhydrous hexanes. The PS–COCl or dPS–COCl product was dried under vacuum to preclude contact with water. To estimate the degree of

Table 1
Characteristics of the polymers employed by this study

Polymer	M_w/kDa	M_w/M_n	% Functionalized
dPS–COOH	58.3	1.05	>95
PS–COOH	50.4	1.05	>95
PS	59.0	1.06	0
$PMMA–NH_2$	34.5	1.13	>90
PMMA–OH	37.1	1.06	>90

Table 2
Characteristics of the bilayer systems investigated

System	h_{PS}/nm (top)	h_{PMMA}/nm (bottom)	$scCO_2$	Functional polymers in top/bottom layer
A	140	60	Yes	dPS–COCl/PMMA–NH_2
B	127	66	Yes	PS–COCl/PMMA–NH_2
C	112	64	Yes	–/PMMA–NH_2
D	121	62	No	PS–COCl/PMMA–OH
E	109	62	No	–/PMMA–OH

conversion of the end groups, oligomeric PS–COOH (Polymer Source, $M_w = 1.2$ kDa, $M_w/M_n = 1.11$) was dissolved in anhydrous deuterated chloroform at a concentration of ~10 mg/mL. Approximately 100× excess of oxalyl chloride was added and stirred overnight. The solution was analyzed by ^{1}H NMR, as the proton on the α-carbon belonging to the –COOH and –COCl groups is easily resolved for low-molecular-weight PS–COOH and PS–COCl [40]. Quantitative conversion was observed for the oligomeric PS–COOH. Due to the long conversion times used, we assume that similar conversion rates have been achieved for the higher molecular weight PS–COOH as well.

Thin film bilayers were prepared by spin-casting polymer solutions onto either 1×1 cm^2 hydrogen-passivated silicon (100) wafers for SIMS analysis or 2.5×2.5 cm^2 wafers for XR characterization. PMMA–NH_2 (*A*, *B* and *C*) or PMMA–OH (*D* and *E*) was dissolved in anhydrous toluene (Fisher Scientific) and spun-cast to a thickness (*h*) of ≈60–65 nm, as determined by ellipsometry. The films were annealed under vacuum at 135 °C for 30 min. For systems *A*, *B* and *D*, a mixture of 19 vol% dPS–COCl (*A*) or PS–COCl (*B* and *D*) and 81 vol% PS was dissolved in 1-chloropentane (Fisher Scientific) that had been stirred over calcium chloride for 6 h [41]. The reactive PS/PS–COCl solution was spun-cast directly onto the PMMA–NH_2 (*A* and *B*) or PMMA–OH (*D*) layer. Note that PMMA has been found to be completely immiscible in 1-chloropentane. Unreactive reference samples (*C* and *E*) were prepared by casting nonfunctional PS directly onto PMMA–NH_2 (*C*) or PMMA–OH (*E*) using 1-chloropentane. Sample *A* had a PS layer with $h \approx 140$ nm as measured with ellipsometry, whereas 'PS' layer thickness for systems *B*–*E* was determined using XR with $h \approx 120$ nm (for details see Table 2). Bilayers of *A* were annealed for 2, 4, and 6 h at 50 °C and 9.6 MPa, as well as 5 and 7 h at 36 °C and 8.2 MPa at the Garcia MRSEC (SUNY, Stony Brook). Systems *B* and *C* were annealed for 5 h at 50 °C and 9.9 MPa in a high-pressure cell in the presence of $scCO_2$ and then rapidly quenched to atmospheric pressure [42–44]. Bilayers of system *D* and *E* were annealed under vacuum at 140 °C for 20 h and 160 °C for 18 h, respectively.

2.2. SIMS

The deuterium depth profiles of system *A* were acquired using a CAMECA IMS-6F magnetic sector spectrometer operated with a 15 nA Cs^+ primary beam (6.0 keV impact energy) that was rastered over a 200×200 μm^2 area. Negative secondary ions were detected from a 60 μm circular optically gated area positioned in the centre of the raster. A sacrificial PS top layer (70 nm) was added after the reaction to ensure uniform ion sputtering throughout the sample, and a 20 nm gold coating was deposited on top of the sacrificial layer to eliminate charge build-up. The analysis conditions were optimized to provide a nominal depth resolution of 5 nm.

2.3. X-ray reflectivity

The XR measurements were conducted at beamline X10B at the National Synchrotron Light Source, Brookhaven National Laboratory, using a photon energy of 14 keV (i.e. X-ray wavelength $\lambda = 0.87$ Å). The specularly reflected intensity was measured by varying α_i and α_f while maintaining the condition $\alpha_i = \alpha_f$ (α_i and α_f denote the incident and reflected angles, respectively). Because the specular reflectivity, presented as scattered intensity versus scattering vector $q_z = (4\pi/\lambda)\sin\alpha_i$, detects the variation of electron density along the surface normal, it is sensitive to *h*, density ρ, interfacial width *w*, and surface roughness σ. However, in the case of XR analysis of polymer bilayer systems, difficulties often arise in obtaining details regarding polymer–polymer interfaces due to the small X-ray contrast between the individual polymers [45], which is typically less than 10% for most polymer pairs [46]. To overcome this difficulty, we used a Fourier transformation (FT) analysis method developed previously [45]. A four-layer model (i.e. Si substrate, native oxide layer, PMMA layer, and PS layer) was used to fit the XR data.

3. Results and discussion

To provide direct observation of BCP formation and progression over time, real-space deuterium depth profiles of system *A* have been generated using SIMS. These profiles, after reaction in $scCO_2$ at 50 °C and 9.6 MPa (Fig. 2), have been analyzed by fitting them to two Gaussian error functions for the underlying dPS–COCl profile and a superimposed Gaussian peak to account for dPS-*b*-PMMA formation at the interface using a Levenberg–Marquardt minimization algorithm [47]. The full width at half maximum of the Gaussian corresponding to the error function profile was used as a measure of the depth resolution (~5 nm). The area under the Gaussian peak yields the interfacial excess (Z^*) according to the analytical solution [27]

$$Z^* \equiv \left(\frac{\pi}{4 \ln 2}\right)^{1/2} \varphi_p \Delta \quad (1)$$

where φ_p is the height and Δ is the full width at half maximum of the Gaussian peak. The total area under the

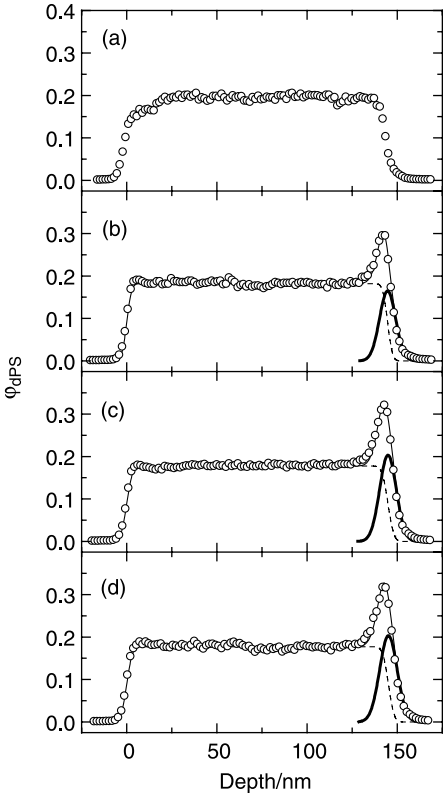

Fig. 2. SIMS depth profiles of system *A* after reaction at 50 °C and 9.6 MPa $scCO_2$ for (a) 0, (b) 2, (c) 4, and (b) 6 h. Each profile represents the dPS volume fraction (ϕ_{dPS}) as a function of specimen depth (Z) normal to the polymer–air interface (at $Z=0$) and traces the concentration of dPS and, thus, also the dPS-*b*-PMMA reaction product. The area under the Gaussian peak yields the interfacial excess (Z^*) according to Eq. (1).

profile is constrained by the initial dPS–COCl concentration and top layer thickness.

A normalized interfacial excess (Z^*/R), where R denotes the RMS end-to-end distance [2] of a dPS chain ($R \approx 15$ nm), can be extracted from each of the SIMS profiles shown in Fig. 2. The excess is presented as a function of reaction time (t) in Fig. 3. The time dependence of Z^*/R can be represented by an empirical expression [26] of the form

$$\left(\frac{Z^*}{R}\right) = \left(\frac{Z^*}{R}\right)^{\infty}\left[1-\exp(-t/\tau)\right] \quad (2)$$

According to the regressed fit of Eq. (1) to the data in Fig. 3, the interface appears to saturate at $(Z^*/R)^{\infty}=0.17$, and the characteristic reaction time (τ) for diblock copolymer formation for this system at 50 °C and 9.6 MPa $scCO_2$ is 1.5 h. Although the physical ramifications of Eq. (2) in the present study are not yet fully established, this relationship has been reported by Jiao et al. [26] with regard to interfacial reactions at 170–190 °C in planar films composed of dPS–NH_2 and a random copolymer of styrene and maleic anhydride. It is intriguing to note that, while the reactions presented here have been performed at much lower temperatures, τ is comparable in magnitude to the

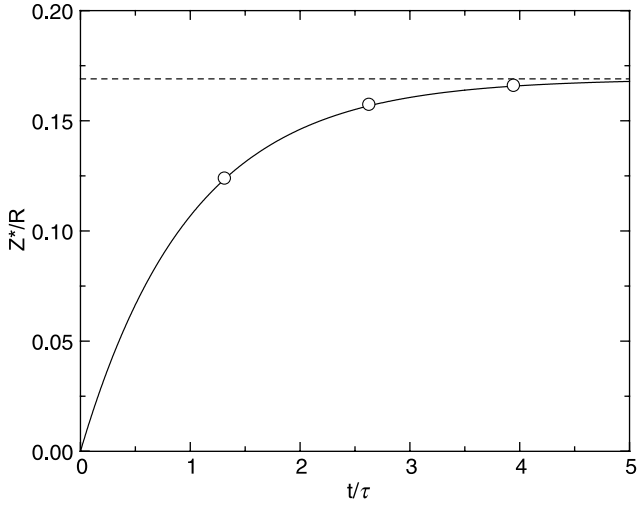

Fig. 3. Normalized interfacial excess Z^*/R presented as a function of residence time (t) scaled with respect to the characteristic reaction time ($\tau=1.5$ h). The SIMS data collected from reactions performed in $scCO_2$ (50 °C and 9.6 MPa) are shown as (○). The regressed fit to Eq. (2) (solid line) indicates that the reaction follows a kinetic expression with an asymptotic limit (dashed line) of $Z^*/R=0.17$.

values measured by Jiao et al. for comparable molecular weight systems with stable interfaces [26]. Although this comparison is rather qualitative, it nonetheless validates the progression of our low-temperature macromolecular reaction and points to similarities to systems reacted in the melt.

The strength of the NH_2/COCl reaction at the interface is most evident with system *A* after exposure to $scCO_2$ at 36 °C and 8.2 MPa. The SIMS depth profiles presented in Fig. 4 clearly show a diffusion gradient and interfacial excess of BCP. This behavior is indicative of DC reactions [27], which is only possible with very fast, irreversible reactions [48]. Because of the concentration gradient near the interface, determination of Z^* would require detailed knowledge of the diffusion profile and the ability of the interface to act as a truly perfect sink for reaction [27]. The reactive PS is expected to reach the interface ≈50 times faster at 50 °C and 9.6 MPa than at 36 °C and 8.2 MPa according to tracer diffusion constants measured in very thin (∼50 nm) PS films [49]. Therefore, we have been able to traverse from RC-type to DC-type behavior over this small temperature range due to the control over chain mobility by using $scCO_2$ concentration (pressure). This could make $scCO_2$ an extremely useful tool for experimental investigations of DC reactions at polymer–polymer interfaces. It should also be noted that a small, but insignificant, excess is observed at the surface of the PS layer. Although isotopic labeling is known to cause surface segregation of dPS to a PS surface in vacuum in higher molecular weight systems [50], the effects of $scCO_2$ on this phenomenon has yet to be investigated.

The XR measurements performed on systems *B* and *C* confirm that the thin films do not foam during the rapid

Table 3
Preparation conditions and interfacial characteristics of the systems analyzed using XR

System	*T*/°C	*P*/MPa	scCO2	Rx	*t*/h	*w*/nm	σ/nm
B	50	9.9	Yes	–COCl/–NH_2	5	5.6	0.60
C	50	9.9	Yes	No reaction	5	5.6	0.64
D	140	Vac	No	–COCl/–OH	20	4.8	0.56
D	160	Vac	No	–COCl/–OH	18	6.2	0.64
E	140	Vac	No	No reaction	20	4.6	0.36
E	160	Vac	No	No reaction	18	4.6	0.56

depressurization from 9.9 MPa and 50 °C in $scCO_2$ to ambient pressure and temperature (25 °C). This has been witnessed previously for thin PS films [42]. This is clearly indicated by the presence of Kiessig fringes extending to high q_z as shown in the reflectivity profile in Fig. 5, and the small values of *w* and σ measured for *B* and *C* (included in Table 3). These ex situ measurements can be performed using XR because the bilayer and individual polymer properties are frozen-in during depressurization from $scCO_2$ [42,49,51]. No change in interfacial width *w* due to reaction was apparent for system *B* when compared to the unreactive *C*. This is not that surprising given the relatively low BCP concentrations that form at the interface [26,52]. The XR analysis also confirms that sharp interfaces are produced by the direct casting of PS onto PMMA using 1-chloropentane.

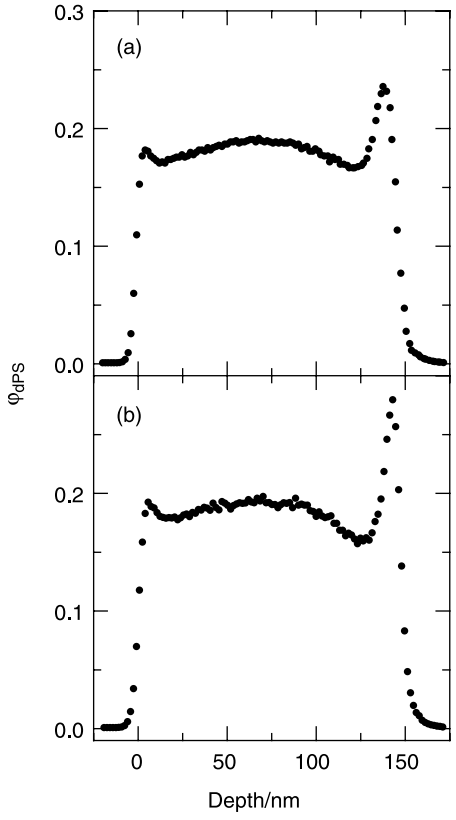

Fig. 4. SIMS depth profiles of system *A* after reaction at 36 °C and 8.2 MPa $scCO_2$ for (a) 5 and (b) 7 h. As in Fig. 2, each profile represents the dPS volume fraction (ϕ_{dPS}) as a function of specimen depth (*Z*) normal to the polymer–air interface (at $Z=0$). The diffusion gradient near the interface is indicative of diffusion-controlled reactions.

In order to make a direct comparison to more traditional systems involving melts at higher annealing temperatures, the PS–COCl/PMMA–OH system (*D*) has been reacted in vacuum at 140 and 160 °C for 20 and 18 h, respectively. The use of –OH termination on the PMMA rather than –NH_2 termination is necessary to prevent a side reaction between the –NH_2 PMMA-end group and the ester side groups along the PMMA main chain [53]. Previously reported investigations [53] have shown that this condensation reaction would be significant at temperatures greater than the intrinsic T_g of the syndiotactic PMMA employed here. This would be a first-order reaction with respect to –NH_2 concentration and, despite the lower reactivity of the ester group, it would become significant due to the very high concentration of ester side groups in the PMMA layer. Annealing at these temperatures could altogether eliminate –NH_2 reactivity in the PMMA layer. As such, the use of PMMA–OH for the high temperature reactions was preventative in nature. The –COCl/–OH condensation reaction is an extremely robust, irreversible reaction [38,54] and is known to produce BCPs at the PS/PMMA interface [27], although the rate of reaction for –COCl/–NH_2 is approximately 50 times greater than that of –COCl/–OH [37]. Compared to the unreactive reference samples (*E*), a negligible change in *w* due to reaction is observed. It is clear from the XR data presented in Table 3 that *w* does not change significantly when pure reference samples (*E*) are compared to systems annealed with or without the addition of $scCO_2$, as well as with or without reaction, for the PS/PMMA systems presented here. Table 3 summarizes measurements of σ and *w* for systems *A*–*E*. The experimental error associated with these values is ~10–15% [45]. Although some variation between measurements of different samples is observed, no systematic or significant changes in *w* can be discerned for the various samples and processing conditions.

4. Conclusions

By detecting an interfacial excess of dPS, we have demonstrated that dPS-*b*-PMMA BCPs form by the interfacial reaction of dPS–COCl and PMMA–NH_2 in the presence of $scCO_2$ at temperatures (36 or 50 °C) far below

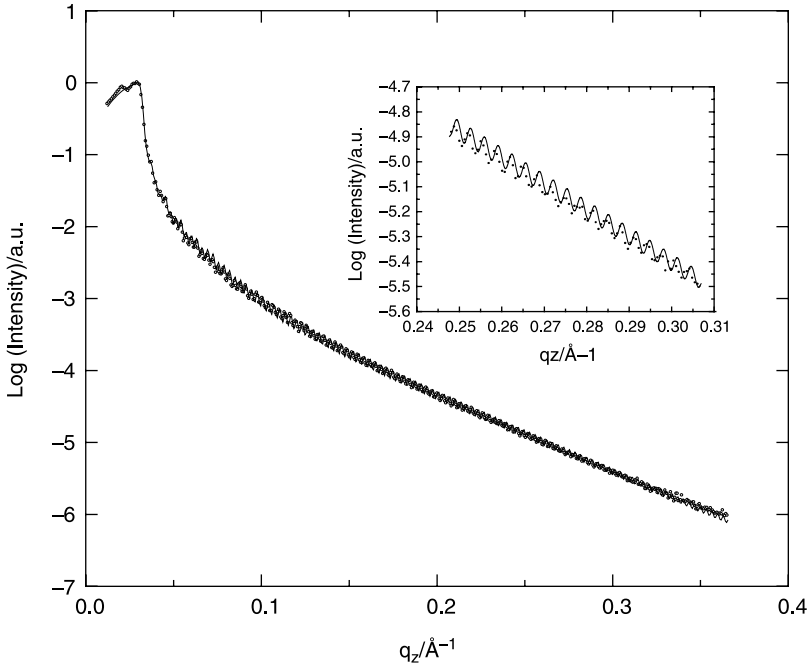

Fig. 5. XR profile of system *C* after reaction for 5 h in $scCO_2$ at 50 °C and 9.9 MPa. The inset shows a small region of the profile to delineate the experimental data points (○) and simulated profile (solid line). The Kiessig fringes at high q_z clearly indicate smooth films with no evidence of foaming.

the intrinsic T_gs of the polymers employed. The addition of $scCO_2$ has been shown to have dramatic effects on reaction behavior. The primary contribution of the $scCO_2$ is increased mobility of the reactive polymer chains due to plasticization [55,56]. The results presented here for a polymer–polymer reaction in a thin film planar geometry are anticipated to extend to comparable polymer–substrate reactions involving an inorganic substrate, as well as to polymer–polymer reactions in nonplanar (curved) dispersions, such as those encountered in commercial extrusion-based processes. This work constitutes the first step in establishing the viability of performing reactive compatibilization in the presence of $scCO_2$. From SIMS analysis of reactions of system *A* performed at two different conditions in $scCO_2$ (50 °C and 9.6 MPa, and 36 °C and 8.2 MPa), we can identify significant changes in reaction progression over time to include changes in the reaction mechanism from reaction- to diffusion-controlled type behavior. This behavior can be attributed to changes in diffusivity of dPS–COCl over this relatively small temperature window. The primary contribution of added $scCO_2$ to the reactive systems presented here, that is, enhanced polymer chain mobility, is directly established.

5. Acknowledgments

This work was supported by the National Science Foundation (DMR-0071743, the Garcia MRSEC, and partially by CHE-9876674, the Center for Environmentally Responsible Solvents and Processes) and the US Department of Energy (DE-FG02-98ER45737). XR experiments were performed at beamline X10B at the National Synchrotron Light Source. We gratefully acknowledge enlightening discussions with Dr Sunil K. Varshney (Polymer Source, Inc) and with Prof B.M. Novak, K. Seto, and Y. Aoyama (NCSU).

References

[1] Ryan AJ. Nat Mater 2002;1:8.
[2] Flory PJ. Principles of polymer chemistry. Ithaca, NY: Cornell University Press; 1953.
[3] Paul DR, Bucknall CB, editors. Polymer blends, vols. I/II. New York: Wiley; 2000.
[4] Utracki LA. Polym Eng Sci 1995;35:2.
[5] Utracki LA. Polymer alloys and blends: Thermodynamics and rheology. Munich: Carl Hanser Verlag; 1990.
[6] Bates FS, Maurer WW, Lipic PM, Hillmyer MA, Almdal K, Mortensen K, et al. Phys Rev Lett 1997;79:849.
[7] Zhu S, Liu Y, Rafailovich MH, Sokolov J, Gersappe D, Winesett DA, et al. Nature 1999;400:49.
[8] Pernot H, Baumert M, Court F, Leibler L. Nat Mater 2002;1:54.
[9] Litmanovich AD, Platé NA, Kudryavtsev YW. Prog Polym Sci 2002; 27:915.
[10] Guégan P, Macosko CW, Ishizone T, Hirao A, Nakahama S. Macromolecules 1994;27:4993.
[11] Walker TA, Raghavan SR, Royer JR, Smith SD, Wignall GD, Melnichenko Y, et al. J Phys Chem B 1999;103:5472.
[12] Elkovitch MD, Lee LJ, Tomasko DL. Polym Eng Sci 2000;40:1850.
[13] Elkovitch MD, Lee LJ, Tomasko DL. Polym Eng Sci 2001;41:2108.
[14] Sundararaj U, Macosko CW. Macromolecules 1995;28:2647.
[15] Macosko CW, Guégan P, Khandpur AK, Nakayama A, Marechal P, Inoue T. Macromolecules 1996;29:5590.
[16] Hadjichristidis N, Pispas S, Floudas GA. Block copolymers. Hoboken, NJ: Wiley-Interscience; 2003.

[17] de Gennes PG. J Chem Phys 1982;76:3322.
[18] de Gennes PG. J Chem Phys 1982;76:3316.
[19] Durning C, O'Shaughnessy B. J Chem Phys 1988;88:7117.
[20] Fredrickson GH. Phys Rev Lett 1996;76:3440.
[21] O'Shaughnessy B, Sawhney U. Phys Rev Lett 1996;76:3444.
[22] O'Shaughnessy B, Sawhney U. Macromolecules 1996;29:7230.
[23] Fredrickson GH, Milner ST. Macromolecules 1996;29:7386.
[24] Fredrickson GH, Leibler L. Macromolecules 1996;29:2674.
[25] O'Shaughnessy B, Vavylonis D. Eur Phys J E 2000;1:159.
[26] Jiao JB, Kramer EJ, de Vos S, Moller M, Koning C. Macromolecules 1999;32:6261.
[27] Harton SE, Stevie FA, Ade H. Macromolecules 2005;38:3543.
[28] Jones TD, Schulze JS, Macosko CW, Lodge TP. Macromolecules 2003;36:7212.
[29] Schulze JS, Cernohous JJ, Hirao A, Lodge TP, Macosko CW. Macromolecules 2000;33:1191.
[30] Schwarz SA, Wilkens BJ, Pudensi MAA, Rafailovich MH, Sokolov J, Zhao X, et al. Mol Phys 1992;76:937.
[31] Kramer EJ. Physica B 1991;173:189.
[32] Orr CA, Cernohous JJ, Guegan P, Hirao A, Jeon HK, Macosko CW. Polymer 2001;42:8171.
[33] Jiao J., PhD Thesis, Cornell University; 1997.
[34] Zheng X, Sauer BB, Alsten JGV, Schwarz SA, Rafailovich MH, Sokolov J, et al. Phys Rev Lett 1995;74:407.
[35] Zheng X, Rafailovich MH, Sokolov J, Strzhemechny Y, Schwarz SA, Sauer BB, et al. Phys Rev Lett 1997;79:241.
[36] Torres JA, Nealey PF, de Pablo J. J Phys Rev Lett 2000;85:3221.
[37] Bentley TW, Llewellyn G, McAlister JA. J Org Chem 1996;61:7927.
[38] Sonntag NOV. Chem Rev 1953;52:237.
[39] Adams R, Ulich LH. J Am Chem Soc 1920;42:599.
[40] Lambert JB, Shurvell HF, Lightner DA, Cooks RG. Organic structural spectroscopy. Simon&Schuster: Upper Saddle River, NJ; 1998.
[41] Burfield DR, Lee K-H, Smithers RH. J Org Chem 1977;42:3060.
[42] Koga T, Seo Y, Jerome J, Ge S, Seek OH, Rafailovich MH, et al. Appl Phys Lett 2003;83:4309.
[43] Koga T, Seo Y-S, Shin K, Zhang Y, Rafailovich MH, Sokolov JC, et al. Macromolecules 2003;36:5236.
[44] Koga T, Seo YS, Zhang YM, Shin K, Kusano K, Nishikawa K, et al. Phys Rev Lett 2002;89 [art. no. 125506].
[45] Seeck OH, Kaendler ID, Tolan M, Shin M, Rafailovich MH, Sokolov J, et al. Appl Phys Lett 2000;76:2713.
[46] Stamm M, Reiter G, Kunz K. Physica B 1991;173:35.
[47] Press WH, Flannery BP, Teukolsky SA, Vetterling WT. Numerical recipes in Fortran 77: The art of scientific computing. 2nd ed. Cambridge: Cambridge University Press; 1992.
[48] O'Shaughnessy B, Vavylonis D. Macromolecules 1999;32:1785.
[49] Koga T, Seo Y-S, Hu X, Shin K, Zhang Y, Rafailovich MH, et al. Europhys Lett 2002;60:559.
[50] Jones RAL, Kramer EJ, Rafailovich MH, Sokolov J, Schwarz SA. Phys Rev Lett 1989;62:280.
[51] Koga T, Jerome JL, Seo Y-S, Rafailovich MH, Sokolov JC, Satija SK. Langmuir 2005;21:6157.
[52] Hayashi M, Grull H, Esker AR, Weber M, Sung L, Satija SK, et al. Macromolecules 2000;33:6485.
[53] Pavlinec J, Lazar M. J Appl Polym Sci 1995;55:39.
[54] Branch GEK, Nixon AC. J Am Chem Soc 1936;58:2499.
[55] Kelley FN, Bueche F. J Polym Sci 1961;50:549.
[56] Wissinger RG, Paulaitis ME. Polym Sci B: Polym Phys 1987;25: 2497.